SUPPLEMENTARY FIGURES

Genome-wide postnatal changes in immunity following fetal inflammatory response

Daniel Costa[1,2], Nuria Bonet[3], Amanda Solé[2,4,5], Jose Manuel González de Aledo[6], Eduard Sabidó[2,4,5], Ferran Casals[3], Carlota Rovira[7], Alfons Nadal[8], Jose Luis Marin[9], Teresa Cobo[9,*], Robert Castelo[2,10,*]

[1]Department of Pediatrics, Hospital de Figueres, Figueres, Spain; [2]Department of Experimental and Health Sciences, Universitat Pompeu Fabra (UPF), Barcelona, Spain; [3]Genomics Core Facility, Department of Experimental and Health Sciences, Universitat Pompeu Fabra (UPF), Barcelona, Spain; [4]Proteomics Unit, Centre de Regulaci Genmica (CRG), Barcelona, Spain; [5]Barcelona Institute of Science and Technology (BIST), Barcelona, Spain; [6]Inborn Errors of Metabolism Section, Laboratory of Biochemistry and Molecular Genetics, Hospital Clnic, Barcelona, Spain; [7]Hospital Sant Joan de Déu; [8]Department of Pathology, Hospital Clnic, Institut dInvestigacions Biomdiques August Pi i Sunyer (IDIBAPS), University of Barcelona, Barcelona, Spain; [9]Hospital Clnic, Institut dInvestigacions Biomdiques August Pi i Sunyer (IDIBAPS), University of Barcelona, Centre for Biomedical Research on Rare Diseases (CIBER-ER), Barcelona, Spain; [10]Research Programme on Biomedical Informatics, Institut Hospital del Mar dInvestigacions Mdiques (IMIM), Barcelona, Spain; *Correspondence: Robert Castelo (robert.castelo@upf.edu), Teresa Cobo (tcobo@clinic.cat)

September 25, 2020

Supplementary Figure 1

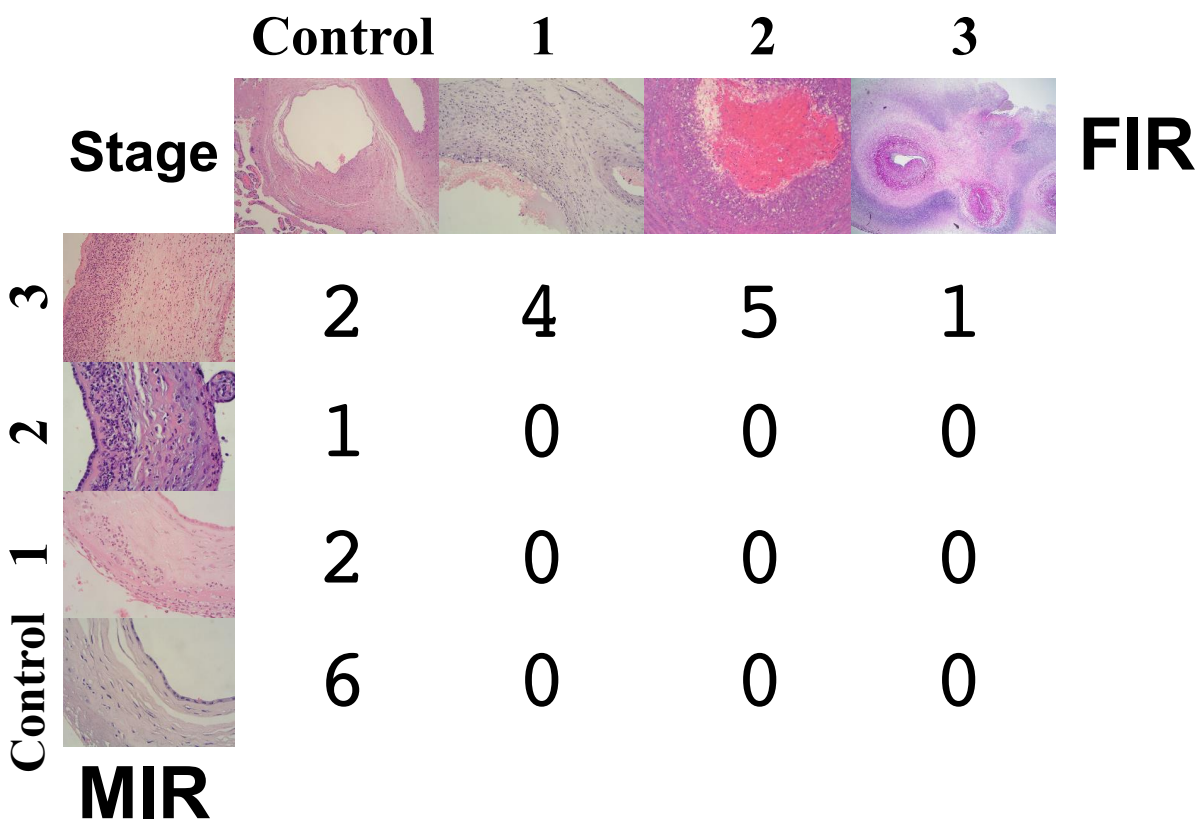

Figure S1 Pathological examination of the placenta. Number of neonates cross-classified by the diagnosis of the stage of the maternal (MIR) and the fetal (FIR) inflammatory response. Original magnifications: MIR Control 40x; MIR Stage 1 20x; MIR Stage 2 40x; MIR Stage 3 20x; FIR Control 10x; FIR Stage 1 20x; FIR Stage 2 40x; FIR Stage 3 2x.

Supplementary Figure 2

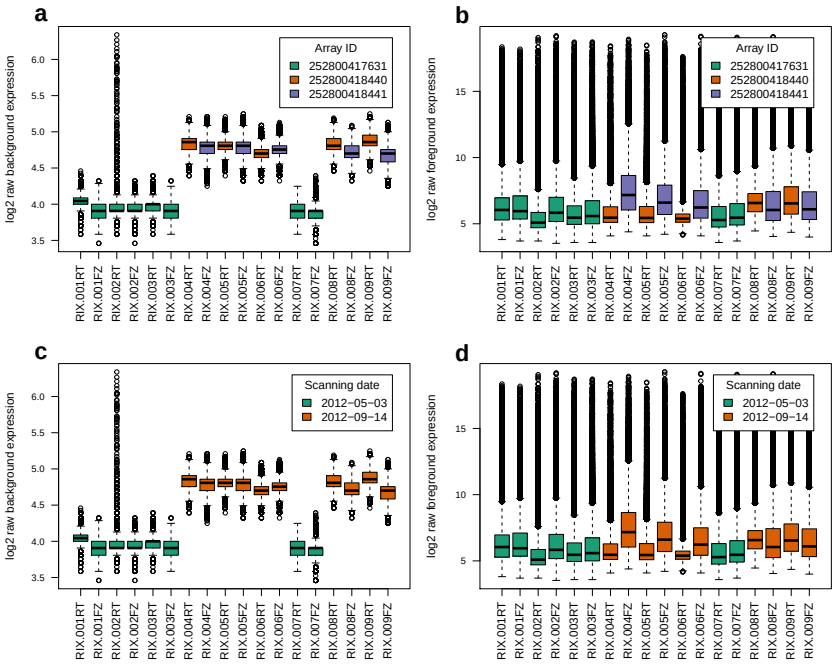

Figure S2 Distribution of raw expression values from the US ELGAN cohort microarray data. (a, c) Expression values from background probes. (b, d) Expression values from foreground probes. (a, b) Samples colored by array identifier. (c, d) Samples colored by scanning date.

Supplementary Figure 3

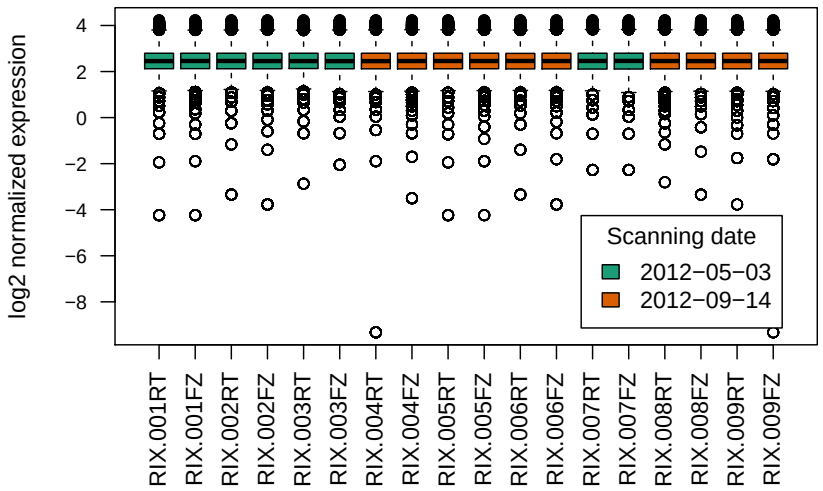

Figure S3 Distribution of background-corrected and quantile-normalized expression values from the US ELGAN cohort microarray data.

Supplementary Figure 4

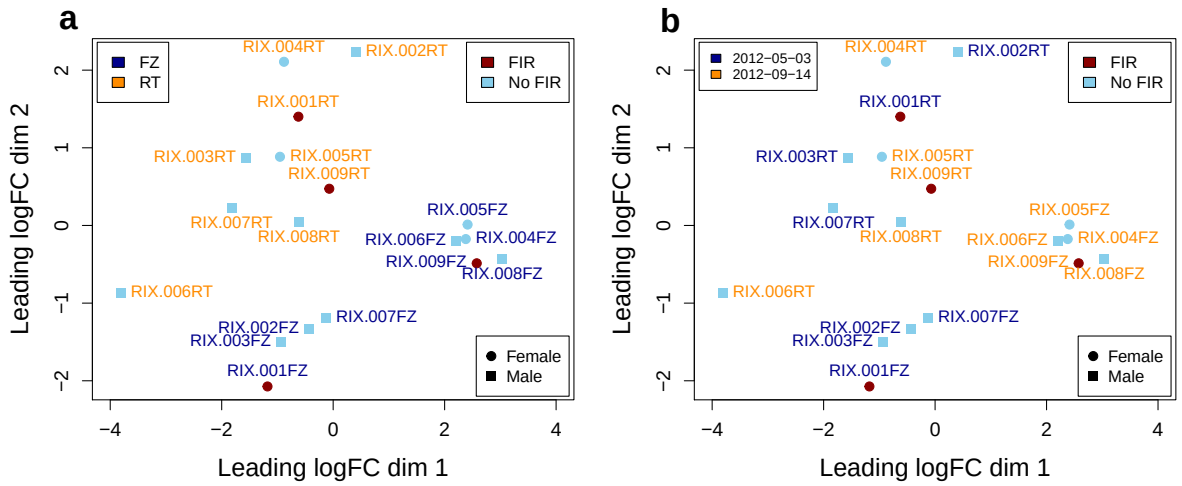

Figure S4 Sample differences from the US ELGAN cohort microarray data, in terms of fold-changes between samples in base-2 logarithmic scale. (a) Sample labels are colored by storage condition (FZ: frozen; RT: room temperature). (b) Sample labels are colored by microarray scanning date. There is a clear effect of storage condition, an effect of scanning date mostly in frozen samples and no apparent sex or FIR effect.

Supplementary Figure 5

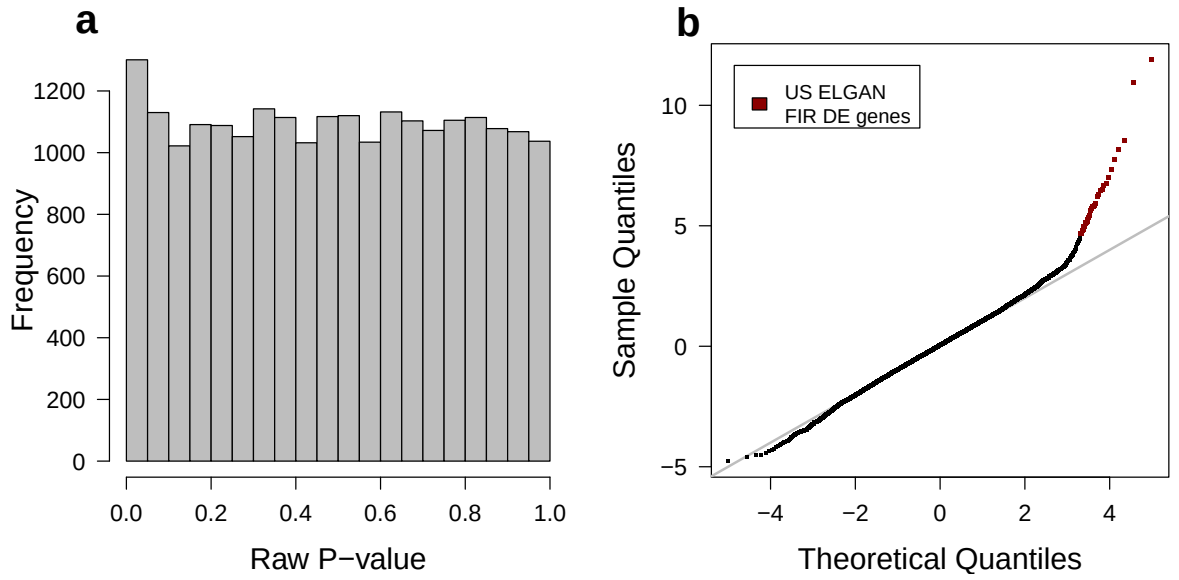

Figure S5 Differential expression between FIR and non-FIR samples from the US ELGAN cohort microarray data. (a) Distribution of raw p-values (b) Quantile-quantile plot of moderated t-statistics.

Supplementary Figure 6

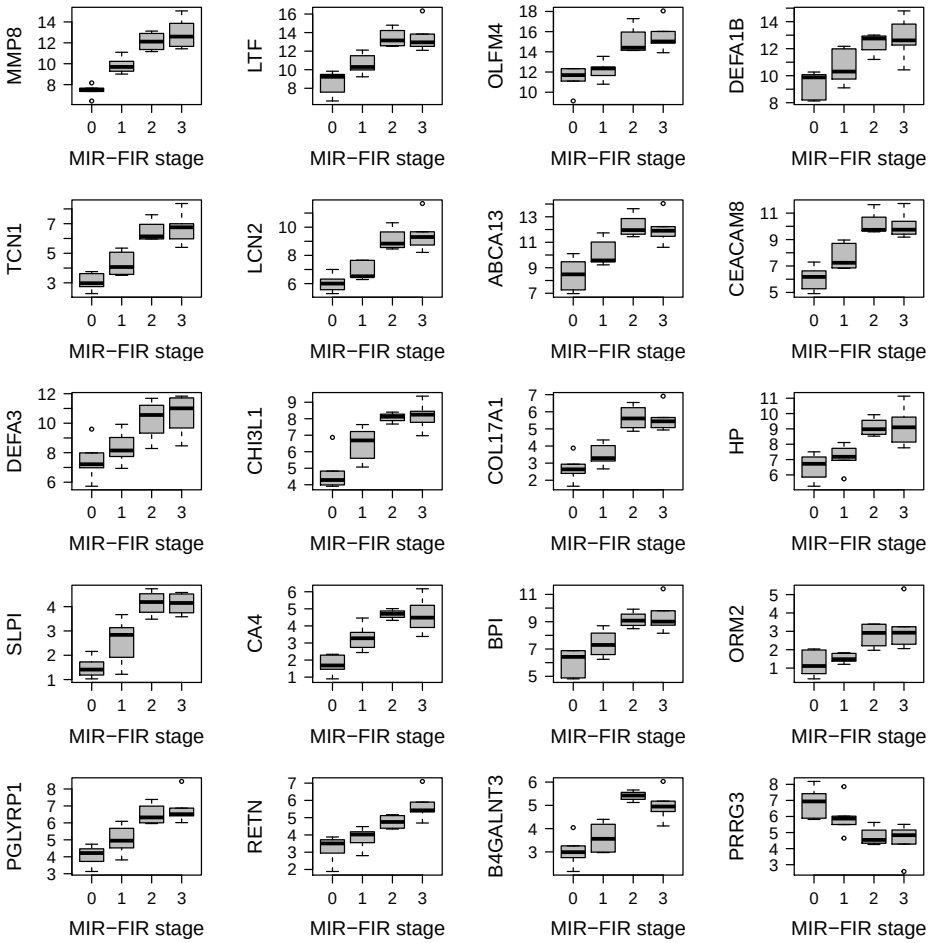

Figure S6 Combined MIR and FIR linear effect on gene expression. Top-20 genes with largest fold change among DE genes with FDR< 5% and minimum-50% fold change throughout the following combined 4 stages of MIR and FIR: 0 no MIR and no FIR; 1 MIR but no FIR; 2 MIR stage 3 and FIR stage 1; 3 MIR stage 3 and FIR stage 2 or 3. Adjusted expression values in log-CPM units are plotted in the y-axis as function of the combined stages in the x-axis.